Ionospheric modification from under-dense heating by high-power HF transmitter

Spencer Kuo,[1] Arnold Snyder,[2] Evgeny Mishin,[3] Paul Kossey,[3] and James Battis[3]

[1] Under-dense HF heating experiments were conducted near local solar noon as well as in the nighttime with the HF heater transmitting at 9.1 MHz directed along the geomagnetic zenith and run at 2 min on and 2 min off. The effective isotropic radiated power of the HF transmitter exceeded 3 GW. The Digisonde operated in a fast mode was used to monitor the temporal evolution of the ionospheric electron density distributions in the bottomside of the ionosphere (in the ranges from 90 to 190 km in the noontime and from 230 to 350 km in the nighttime). The electron temperature distributions were then evaluated. The results show that the electron density distributions are modified continuously over the experimental periods. In the noontime, the electron density decreases/increases in time in the region below/above a height at about 140 km, manifesting the change of the balance between the photoionization and the electron-ion recombination and the electron-oxygen dissociative attachment losses by the heating. In the nighttime, the ionosphere was lifted by 30 to 50 km through continuously upward expansion, resulting in the drop of the electron density in the bottomside of the ionosphere in time. A comparison with the ionogram, height, and electron density distribution of unheated ionosphere with similar background conditions further elaborates the observation of thermal expansion.

1. Introduction

[2] The Ionospheric Research Instrument (IRI) of the High Frequency Active Auroral Research Program (HAARP) is a HF transmitter, which delivers 0.36 to 3.6 GW effective isotropic radiated powers (EIRP) for the radiation frequencies from 2.8 to 10 MHz. The power density of the HF wave in the ionosphere is up to about 30 mW/m^2 at 100 km altitude. It is anticipated that the HF heating of the ionosphere via both collision and collisionless heating processes will make a significant impact on the plasma dynamics of the ionosphere [*Fejer*, 1979; *Gurevich*, 2007; *Kuo et al.*, 2009; *Pedersen et al.*, 2009; *Kuo et al.*, 2010; *Kuo and Snyder*, 2010], which provides useful information for studying the properties and behavior of the ionosphere.

[3] In the past, most of the HF heating experiments were focused on overdense situation by applying O mode HF heaters with frequencies less than the foF2. In this situation, parametric instabilities can be excited locally near or below the HF reflection height to contribute to anomalous heating, where the frequency and wave vector matching conditions for parametric coupling can be satisfied [*Fejer*, 1979; *Stenflo*, 1985; *Kuo*, 2001]. Parametric instabilities have been responsible for the observation of new physical phenomena in the experiments [*Gordon and Carlson*, 1974; *Stubbe et al.*, 1984, 1992]. Moreover, the anomalous heating expanding along the geomagnetic field may cause ionospheric modification over a large altitude region. In particular, by combining solar illumination in the solar noon time period with the anomalous heating of the HF heater, significant modification of the ionospheric plasma density distribution was observed [*Kuo and Snyder*, 2010], which could impact communication systems.

[4] In the case of under-dense heating, the EIRP of the HAARP heater can be increased significantly by increasing the heater frequency. With higher heater frequency, the loss of heating power in the D region, in the daytime experiment, is also reduced. In the daytime, it is anticipated that the electron heating will reduce the electron-ion recombination coefficient to increase the plasma density, provided that transport is insignificant. However, in the E region the rate of attachment of electrons to oxygen can also be increased, resulting in decreasing plasma density. In the nighttime, the ionosphere may be modified via thermal expansion. Therefore, the modification of the ionosphere via overdense and under-dense HF heating as well as in the daytime and nighttime can be quite different.

[5] This work reports experiments conducted with the 9.1 MHz HF heater that explores the under-dense heating effects on the ionospheric electron density distributions in

[1]Department of Electrical and Computer Engineering, Polytechnic Institute of New York University, Brooklyn, New York, USA.
[2]NorthWest Research Associates, Stockton Springs, Maine, USA.
[3]Space Vehicles Directorate, Air Force Research Laboratory, Hanscom Air Force Base, Massachusetts, USA.
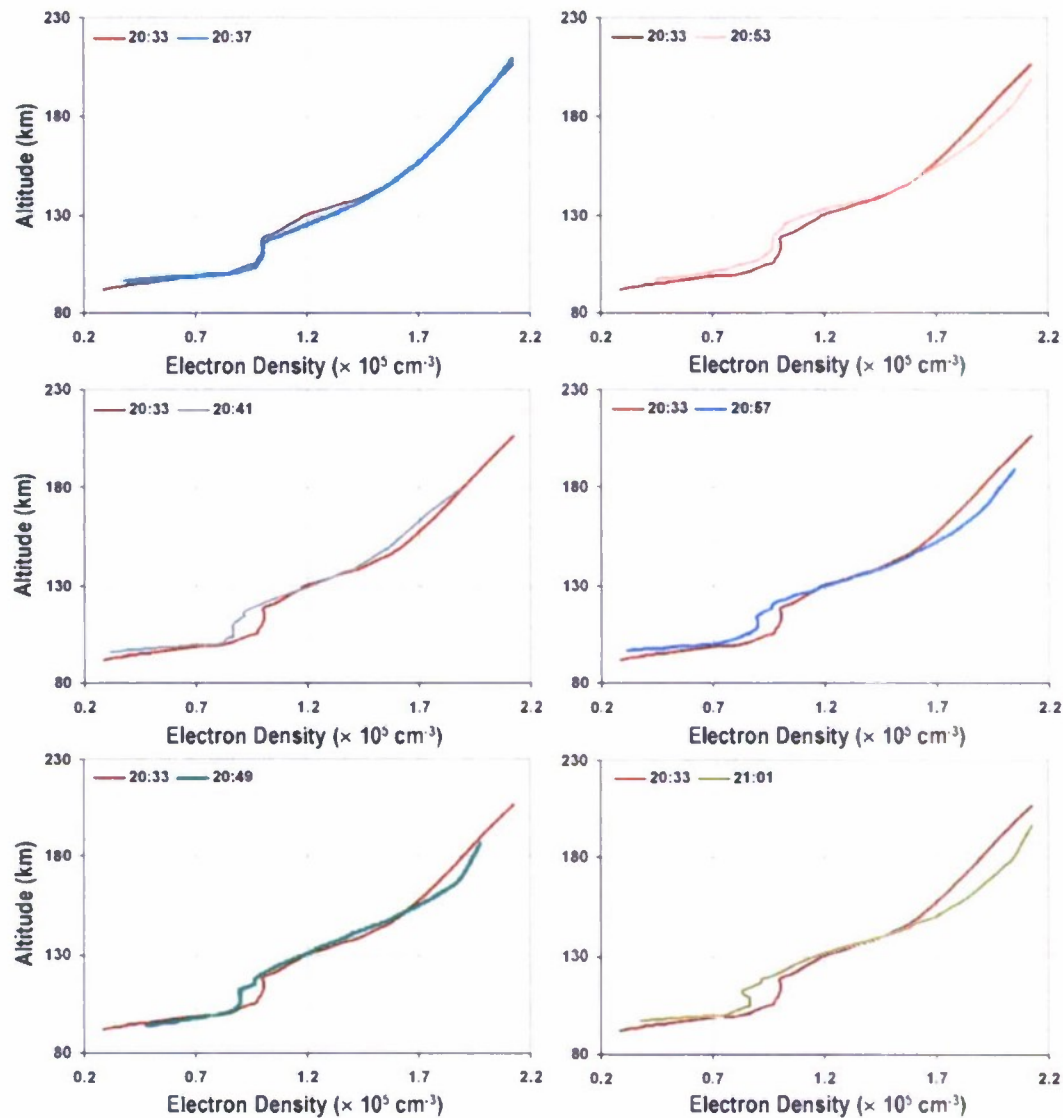
Figure 1. Comparison of common (to on/off) electron density distributions with consecutively increasing heating times. The one corresponding to the first on/off period from 2032 to 2036 UTC is used as a reference.

the solar noon time period and in the nighttime for a comparison. The inelastic collision processes are revealed via the change of the electron density distribution in the noon-time heating experiment.

2. Experiment

[6] On 12 April 2010 from 2032 to 2104 UTC (1232 to 1304 local time) and on 13 April from 0812 to 0844 UTC (0012 to 0044 local time), using the HAARP transmitter facility at Gakona, AK, at full power (3.6 MW), experiments were conducted with the HF heater transmitting at 9.1 MHz directed along the geomagnetic zenith and run at 2 min on and 2 min off. In the on periods, the polarization of the heating wave was switched alternately with O mode and X mode. The 12 × 15 array of the transmitter was split into two

6 × 15 subarrays; one was run at ew full power and the other run at 100% power modulation (PM) by rectangular waves of 2.02 kHz, 5 kHz, 8 kHz, and 13 kHz. Each modulation frequency was applied consecutively in two 2 min on periods at the sequence of O/X mode heater and of 100% power modulation to one of the subarray. The purpose of modulation is to generate VLF wave by wave beating through the nonlinearity of plasma. While the unexpected high-level background noise at 13 kHz contaminated VLF data, new phenomena directly related to HF heating of the background plasma were observed. These new phenomena do not depend on the polarization of the HF heater because the heater frequency is much larger than the peak plasma frequency (foF2). The experiment was monitored by the HAARP Digisonde. The results developed from the ionogram data files are presented.
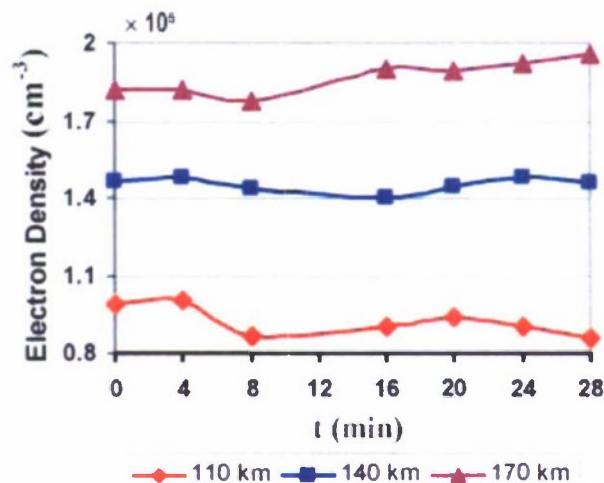
Figure 2. Time evolution of the electron density at three heights: 110, 140, and 170 km in the noontime experiment.

[7] The Digisonde acquired ionograms every minute during the heater on and off periods. The 1.0 to 5.5 MHz ionograms, with 75 kHz steps, started on the minute. The recording of each ionogram took less than 19 s. Thus, the ionogram acquisition time from approximately 2 to 4.6 MHz, the frequency band of interest, was less than 11 s.

3. Experimental Results

3.1. Noontime Experiment

[8] Quantitative frequency distribution and time variations of the virtual height and height spread of the sounding echoes can be examined from the ionogram data files. It was found that during the experiment, the virtual height traces of the echoes in the ionograms were modified continuously. HF heater changed the virtual height and spread of the sounding echoes. In the analysis, we choose data only from the vertical O mode sounding echoes. We divide the O mode sounding echoes in each pair of heater on/off ionograms into three groups. These three groups are (1) unique off ionogram echoes, which appear only in the heater-off ionograms; (2) unique on ionogram echoes, which appear only in the heater-on ionograms; and (3) common ionogram echoes, which appear in both the heater-on/off ionograms being compared. The unique on/off echoes are the additional spread echoes in virtual height to those of the common echoes in the heater-on/off periods. Their difference manifests the heater induced change of density irregularities which are present in the background plasma. The virtual height of the strongest received signal at each frequency is then taken to obtain the frequency distribution of the virtual height of the common echoes in each on-off ionogram pair.

[9] The virtual height distribution of the O mode sounding echo does not represent the actual height distribution of the ionospheric plasma. The University of Massachusetts developed Digisonde provides a software program SAO Explorer [*Galkin et al.*, 2008] (see http://ulcar.uml.edu/ SAO-X/SAO-X.html) for rescaling of the virtual height trace $h'(f)$ and calculation of the true height profile $h(f)$. This program is used to convert a virtual height distribution of common ionogram echoes to a true height distribution versus frequency, which is then inverted to the dependence of electron density on altitude.

[10] The common electron density distributions in the 8 on/off periods are evaluated from the data files of common ionogram echoes. The one corresponding to the first on/off period from 2032 to 2036 UTC was used as a reference for showing the temporal evolution of the electron density distribution in the subsequent on/off periods. As shown in Figure 1, the common electron density distribution evolves continuously in time. It suggests that the heater-induced modification of the electron density distribution lasts longer than the 2 min off period, and the modification accumulates in time. It also shows that after a few on/off periods, the density profile reaches a stable feature; the electron density becomes lower/higher than that of the reference in the lower-/higher-altitude regions.

[11] The temporal evolution of the electron densities at three representative altitudes: 110, 140, and 170 km, is presented in Figure 2 to show the contrast of density changes in time. As shown, the density at 110/170 km decreases/ increases with time after a transient period and the density at 140 km varies slightly around a constant level. The unique on/off echoes are the additional echo spreads from the common echoes in the on/off situations and their difference manifests the heating effect. Thus the frequency dependencies of the virtual heights of the unique on/off echoes are also converted to the frequency dependencies of the true heights of the unique on/off echoes, which determine the electron densities at the true heights of the unique on/off echoes. Combining the electron densities at the true heights of the common echoes and of the unique on/off echoes, we have generated "modeled" electron density distributions at heater on/off, which contain spatial density variations giving "equivalent effects" on the virtual height spreads of the sounding echoes. Normally, one can choose a single virtual height for each strongest received signal at each frequency to obtain a frequency distribution of the virtual height for the unique on or unique off echoes; however, in a few cases observed in the present experiment, the virtual height of the strongest received signal has double values with large height separations. This is demonstrated in Figure 3a, which suggests that the ionosonde can trace more than a single line when the ionospheric density distribution does not have a sharp horizontal layer due to the presence of field-aligned density irregularities. A set of true height results, for the on/ off at 2041/2043 UT, based on the virtual height distributions presented in Figure 3a is presented in Figure 3b. As shown, the heater has modified the magnitude and the scale length of the effective electron density variations of the modeled electron density distributions, which are in quasiperiodic forms resembling density irregularities. Note that each line in Figure 3b intersects with a horizontal line only once; thus, these plots show only density variations in altitude (i.e., in vertical direction). The scale length L of the density variation in vertical direction can be used to determine the scale length L_g of the field-aligned density irregularities by the relation $L_g = L \cos\theta_d$, where θ_d is the magnetic dip angle and equals $76°$ at Gakona, Alaska. The present approach models the heating-induced ionospheric modification manifested by
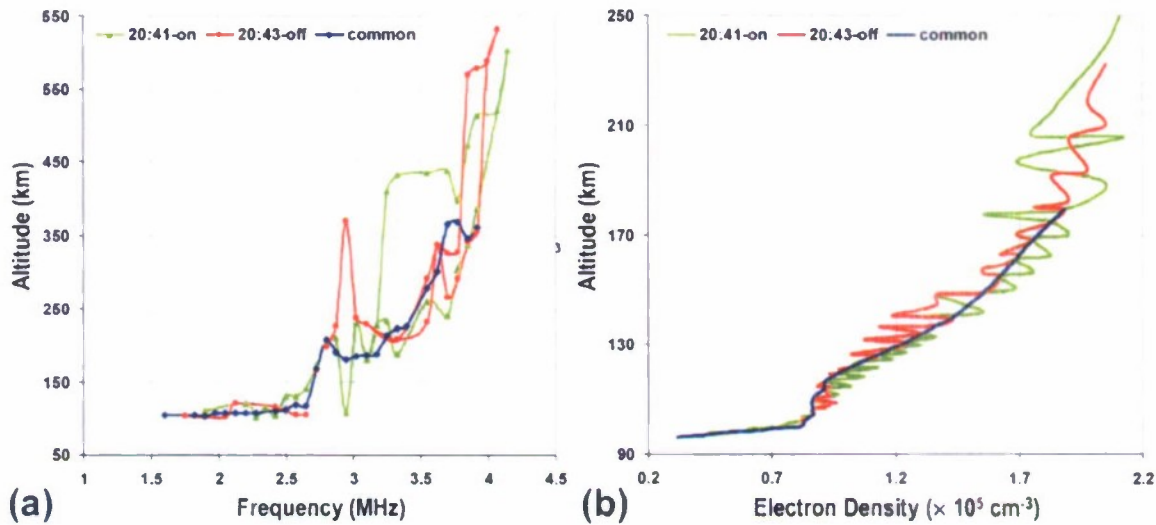
Figure 3. (a) Virtual heights of the strongest unique on/off and common echoes versus the sounding frequency and (b) comparison of the electron density distributions in heater on/off periods, including the common part as a reference.

the virtual height spread of the sounding signal via an equivalent perturbation on the density distribution.

3.2. Nighttime Experiment

[12] The bottomside electron density distributions in the 8 on/off periods from 0812 to 0844 UTC on 13 April are evaluated in the same way. Four of the 16 plots in the X mode heater on periods are presented in Figure 4a to show the temporal evolution of the electron density distribution. As shown the distribution shifts up consecutively with decreasing density as the total heating time increases. The temporal evolutions of electron densities at five heights: 230, 255, 280, 305, and 330 km are presented in Figure 4b. In the initial on/off/on period, the density decreases/increases in the lower/higher altitude; then the trend of density

decreasing in time after this initial period is clearly shown. The transient period covering the first on/off/on suggests that it takes up to 6 min for the ionosphere to reach a steady thermal expansion, which upshifts the ionosphere and continuously depletes the bottomside plasma density. Figure 4b also shows that the densities drop quickly in the beginning, e.g., from 0818 to 0830 UT, and those in the lower altitude reach steady state levels first. This trend is consistent with that in an upward thermally expanding ionosphere.

4. Physical Interpretation

[13] The HF heater of 9.1 MHz cannot excite parametric instabilities for anomalous heating; the wave heating was limited to collisional heating. The electron density distribution
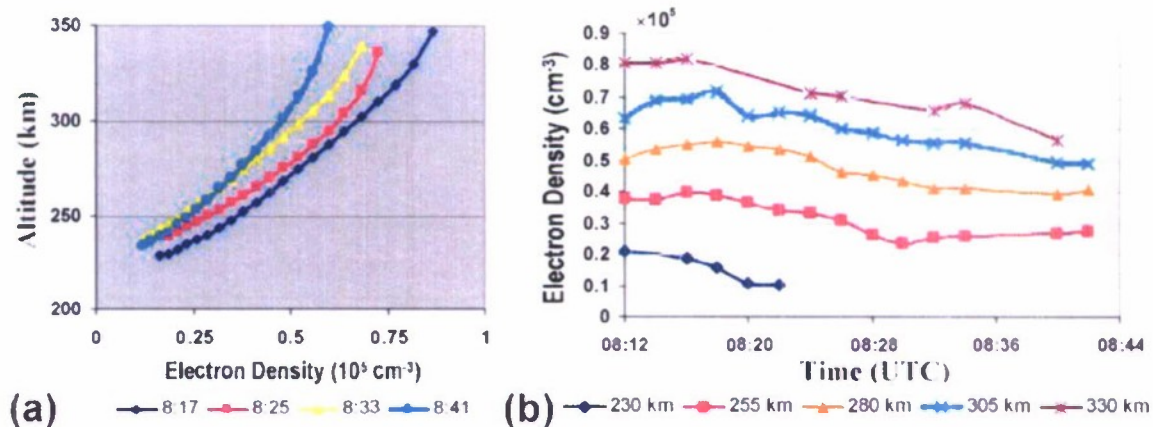

Figure 4. (a) Comparison of electron density distributions with a consecutive increase of the total heating time in the nighttime experiment and (b) time evolution of the electron density at five heights: 230, 255, 280, 305, and 330 km.
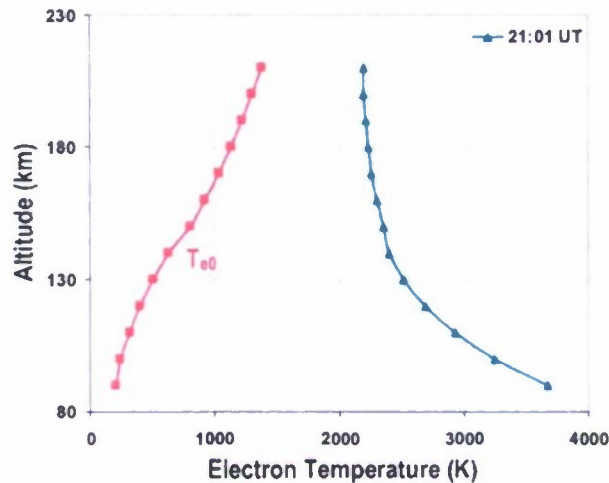
Figure 5. Comparison of the unperturbed electron temperature distribution T_{e0} to that at the end of the noontime heating experiment.

can be modified through two processes: (1) changes of the inelastic collision losses by the heating and (2) thermal expansion along the geomagnetic field.

[14] In the absence of D region absorption, which was the experimental situation, the wavefield intensity E_0 of the HF heater is given by $E_0(z) \sim (3/Z)$ V/m, where $Z = z/z_0$ is the altitude z normalized to a reference height $z_0 = 100$ km. In the steady state, the elevated electron temperature in a circularly polarized heater is given by

$$T_e \sim T_{e0} + 2\ e^2 E_0^2/\left[3\delta(T_e)m\omega^2\right] \qquad (1)$$

where ω is the radian frequency of the heater; $\delta(T_e) = \delta_0 + \delta_{em}$ is the electron energy fraction lost in each collision, here, $\delta_0 = 2m/M$ accounts for elastic collisions and $\delta_{em} = \delta_{em}(T_e)$ accounts for inelastic collisions, which drain electron energy via rotational and vibrational excitations of the neutral molecules (N_2 and O_2). In the strong heating situation, $\delta_{em}(T_e)$ dominates and has to be evaluated self-consistently. With the aid of *Gurevich* [1978, Tables 1, 2, 7, and 8] and the electron density distribution determined by the recorded ionograms, the spatial distribution of T_e is evaluated.

4.1. Processes Involved in Noontime Modifications

[15] Presented in Figure 5 is a comparison of the electron temperature distribution at the end of the heating experiment to the unperturbed distribution T_{e0}, which is based on the values, given by *Gurevich* [1978, Table 2]. As shown, the heater causes a significant increase in the electron temperature, in particular, in the region from 90 to 120 km where the electron density drops by as much as 10%.

[16] Electron heating can also give rise to heating of the neutral gas in terms of populating (vibrationally) excited O_2 and N_2. Consequently, the rates of two inelastic processes may be modified by the heating. One is the electron-ion recombination coefficient, which decreases as the electron temperature increases; the second one is the electron-oxygen

dissociative attachment: $e + O_2 \rightarrow O + O^-$, in which the electron energy has to exceed a threshold level imposed by the conservation of energy. Normally, this threshold is 3.6 eV. However, this threshold level decreases as the internal energy of molecular oxygen increases and the laboratory experimental results [*Henderson et al.*, 1969] show that this threshold can decrease to 1 eV and less. Moreover, an enhancement of the electron attachment coefficient can introduce a focusing effect on the HF heater [*Shukla et al.*, 1992], which further increases the heating and the attachment coefficient. The counterbalance of the two inelastic processes on the electron density gives a net effect on the electron density distribution.

[17] Therefore, a long heating period can change the ionization balance, which involves four processes: (1) photo ionization by the solar illumination, (2) artificial ionization by electrons accelerated by the strong wavefield, (3) electron-heating-caused reduction of the recombination coefficient, and (4) enhancement of the electron attachment coefficient caused by the heating of electrons and oxygen molecules.

[18] The dissociative attachment rate is given by $\nu_a = \sigma N_v v_e$, a product of the cross section σ, density N_v of vibrationally excited molecular oxygen, and the electron velocity v_e, where $v_e \sim 4.2 \times 10^7$ cm/s for a 1 eV electron and the cross section $\sigma \sim 10^{-21}$ cm^2. In the region from 90 to 120 km, $1.2 \times 10^{11} \leq N(O_2) \leq 8.2 \times 10^{12}$ cm^{-3} [e.g., *Gurevich*, 1978, Table 1]; thus, when excited molecular oxygen constitutes a few percent, the total attachment loss of electrons will exceed 10% of its density at the end of the experiment. As the heating wave propagates upward, the wavefield intensity and the background neutral density
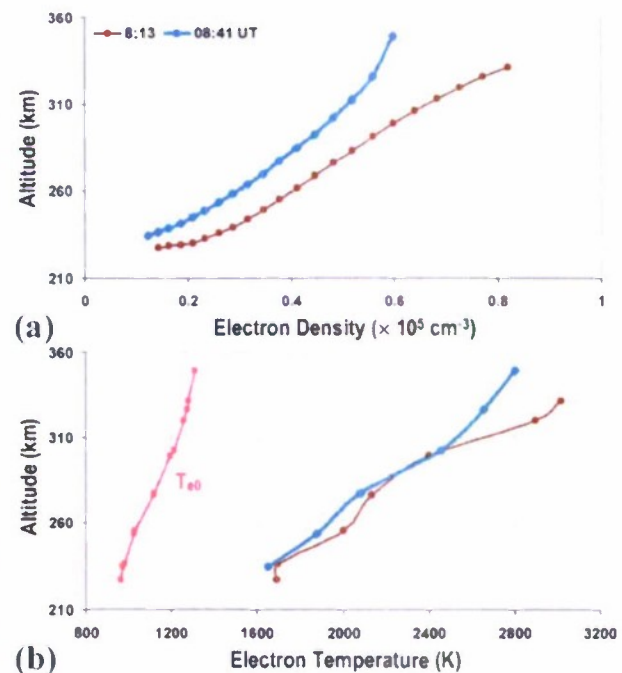

Figure 6. Comparisons of (a) electron density and (b) electron temperature distributions in the beginning and at the end of the nighttime experiment.
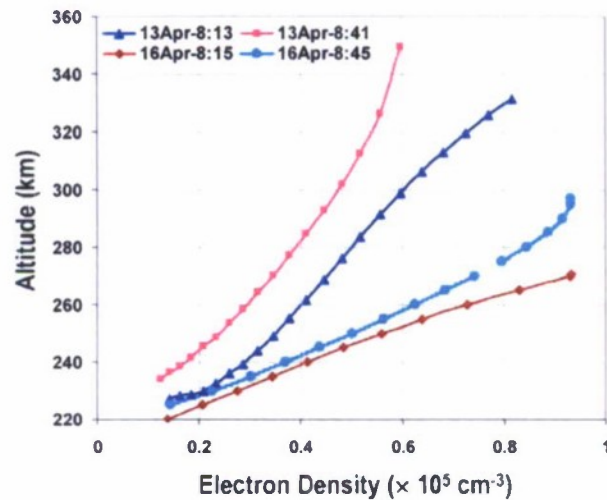
Figure 7. A comparison of the shifts of the electron density distributions on 13 and 16 April, caused by the heating for about 15 min and due to the natural decay of the F layer for 30 min, respectively.

decrease with increasing altitude. Thus the attachment loss rate decreases with the altitude. When the positive change of the attachment rate is larger/smaller (in absolute value) than the negative change of the recombination rate, then the net effect can modify the electron density distribution with depletion in the lower-altitude region and enhancement in the higher-altitude region, as shown in Figure 2.

4.2. Process Responsible for the Nighttime Modifications

[19] Presented in Figures 6a and 6b are comparisons of electron density and temperature distributions in the beginning and at the end of the nighttime heating experiment,

where the elevated electron temperature distributions in Figure 6b were again determined via equation (1). The unperturbed electron temperature T_{e0}, from *Gurevich* [1978, Table 2], is also plotted in Figure 6b as a reference. As shown, the heater causes considerable electron temperature elevation, which remains about the same through the experiment. On the other hand, the electron density decreases continuously in time. In fact, due to the density drop, the heating near foF2 becomes less effective in the later time of the experiment. The results presented in Figure 6 support the thermal expansion explanation on the observation. The background conditions on 13 and 16 April were quite similar as indicated by the magnetometer measurements and no experiment was performed at HAARP on 16 April. Because the natural decay of the F layer as the Sun sets can also cause the decay and upward expansion of the bottomside electron density distribution, the changes of the distributions after 30 min on 13 and 16 April are first compared. As shown in Figure 7, the shift on 16 April was much smaller than that on 13 April. Next, an ionogram recorded on 16 April was taken to compare a corresponding one (i.e., recorded at about the same time of the day) recorded on 13 April in the experiment.

[20] The true height profiles and electron density distributions were also deduced from the two ionograms for a comparison. As shown in Figures 8a and 8b, the virtual heights of the sounding echoes and the true height of the electron density distribution on 13 April are much higher than the corresponding ones on 16 April. The true height profiles of the sounding echoes in Figure 8a were determined by an algorithm that is part of the software program SAO Explorer [*Galkin et al.*, 2008]. The topside profiles in Figure 8a are model results presented for reference only, as the ionosonde cannot observe the topside of the ionosphere. A significant upward expansion of the density distribution on 13 April results in a considerable density drop in the bottomside of the ionosphere. These two comparisons
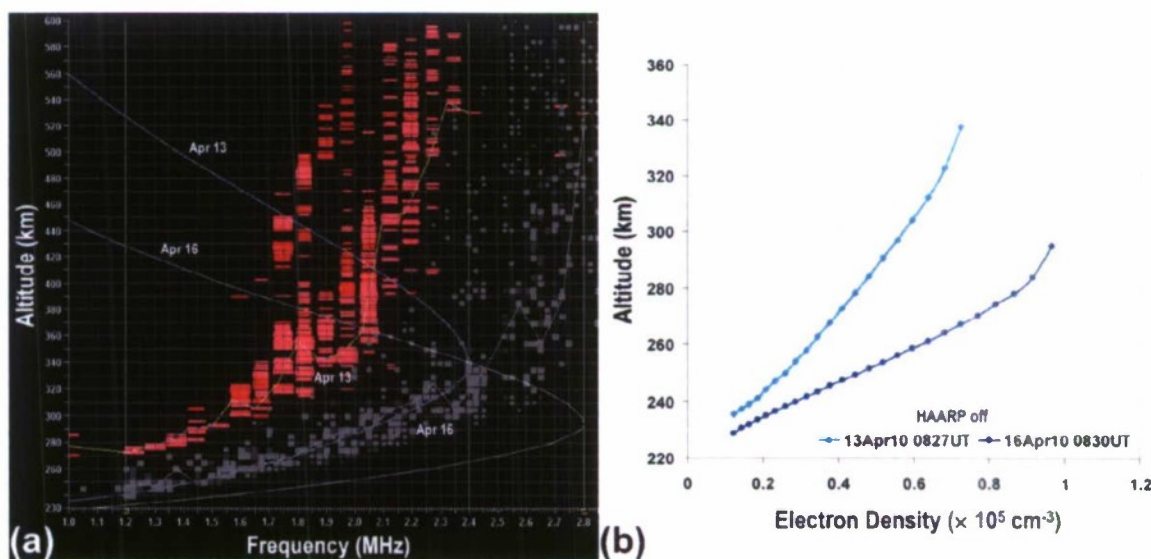

Figure 8. (a) A comparison of the ionograms recorded on 13 and 16 April and (b) the deduced electron density distributions.

clearly demonstrate that the ionosphere on 13 April was lifted mainly by the heating.

5. Discussion

[21] The experimental results show that the impacts of the under-dense heating by a powerful HF wave on the noontime and nighttime ionosphere are quite different from each other as well as different from that of the overdense heating of the ionosphere.

[22] The overdense heating by the O mode HF heater starts locally and involves instabilities, such as parametric instabilities [*Fejer*, 1979; *Stenflo*, 1985] and thermal instability [*Kuo and Djuth*, 1988] and are frequency dependent, such as heating at second harmonic electron cyclotron resonance [*Djuth et al.*, 2005]. Such anomalous heating forms a local heat source which transmits heat both downward and upward through heat conduction along the geomagnetic field. The anomalous electron heating causes a decrease of the recombination rate, which changes the balance between the photoionization and the recombination loss to result in an increase of the electron density. In the process, a thermal instability is also excited to generate large-scale field-aligned density irregularities (FAIs) [*Kuo and Djuth*, 1988], which are responsible for the observed virtual height spread [*Kuo and Snyder*, 2010]. The parametrically excited plasma waves can also resonantly accelerate electrons to exceed 10 eV. *Pedersen et al.* [2009, 2010] suggested those energetic electrons to be the main cause of artificial ionization patches observed in HF heating experiments at HAARP.

[23] On the other hand, the under-dense heating covers a large altitude region from the beginning; EIRP of the heater is probably the most important ingredient. Both bottomside and topside of the ionosphere can be perturbed simultaneously. It causes a larger-scale ionospheric modification which also lasts longer. The experimental results show that the heating effect accumulates in time even in the intermittent heating situation with a 2 min heater-off period introduced between two 2 min heater-on periods.

[24] In the noontime, the ionosphere is at a low altitude; thus, collisions are dominated by the inelastic processes. On the other hand, elastic collisions dominate in the nighttime. Therefore, the electron temperature elevation in noontime under-dense heating decreases with an increase in altitude and the trend is reversed in the nighttime. The electron temperature increases significantly in both experimental time periods. The results of the noontime experiment show that the electron density decreases/increases in time in the region below/above a critical height at about 140 km, manifesting a change of the balance between photoionization and recombination and attachment losses by the heating. The results of the nighttime experiment show that the ionosphere was lifted by 30 to 50 km through continuously upward expansion. In the future work, a numerical simulation effort, similar to that [*Eliasson and Stenflo*, 2010] for the phenomena explored in the overdense heating case, is also called for.

References

Djuth, F. T., T. R. Pedersen, E. A. Gerken, P. A. Bernhardt, C. Selcher, W. A. Bristow, and M. J. Kosch (2005), Ionospheric modification at twice the electron cyclotron frequency, *Phys. Rev. Lett.*, *94*(12), 125001, doi:10.1103/PhysRevLett.94.125001.

Eliasson, B., and L. Stenflo (2010), Full-scale simulation study of stimulated electromagnetic emissions: The first ten milliseconds, *J. Plasma Phys.*, *76*, 369, doi:10.1017/S0022377809990559.

Fejer, J. A. (1979), Ionospheric modification and parametric instabilities, *Rev. Geophys.*, *17*, 135, doi:10.1029/RG017i001p00135.

Galkin, I. A., G. M. Khmyrov, B. W. Reinisch, and J. McElroy (2008), The SAOXML 5: New format for ionogram-derived data, in *Radio Sounding and Plasma Physics*, AIP Conf. Proc., *974*, 160.

Gordon, W. E., and H. C. Carlson (1974), Arecibo heating experiments, *Radio Sci.*, *9*, 1041, doi:10.1029/RS009i011p01041.

Gurevich, A. V. (1978), *Nonlinear Phenomena in the Ionosphere*, chap. 2, Springer, New York.

Gurevich, A. V. (2007), Nonlinear effects in the ionosphere, *Phys. Uspekhi*, *50*, 1091, doi:10.1070/PU2007v050n11ABEH006212.

Henderson, W. R., W. L. Fite, and R. T. Brackmann (1969), Dissociative attachment of electrons to hot oxygen, *Phys. Rev.*, *183*, 157, doi:10.1103/PhysRev.183.157.

Kuo, S. P. (2001), Cascade of the parametric decay instability in ionospheric heating experiments, *J. Geophys. Res.*, *106*(A4), 5593, doi:10.1029/2000JA000240.

Kuo, S. P., and F. T. Djuth (1988), A thermal instability for the spread F echoes from the HF-heated ionosphere, *Geophys. Res. Lett.*, *15*, 1345, doi:10.1029/GL015i012p01345.

Kuo, S. P., and A. Snyder (2010), Observation of artificial Spread-F and large region ionization enhancement in an HF heating experiment at HAARP, *Geophys. Res. Lett.*, *37*, L07101, doi:10.1029/2010GL042656.

Kuo, S. P., W.-T. Cheng, J. A. Cohen, R. Pradipta, M. C. Lee, S. S. Kuo, and A. Snyder (2009), Simultaneous generation of large-scale density irregularities and geomagnetic pulsations via filamentation instability, *Geophys. Res. Lett.*, *36*, L09107, doi:10.1029/2009GL037942.

Kuo, S. P., W.-T. Cheng, A. Snyder, and P. Kossey (2010), Contrasting O/X-mode heater effects on O-mode sounding echo and the generation of magnetic pulsations, *Geophys. Res. Lett.*, *37*, L01101, doi:10.1029/2009GL041471.

Pedersen, T., B. Gustavsson, E. Mishin, E. MacKenzie, H. C. Carlson, M. Starks, and T. Mills (2009), Optical ring formation and ionization production in high power HF heating experiments at HAARP, *Geophys. Res. Lett.*, *36*, L18107, doi:10.1029/2009GL040047.

Pedersen, T., B. Gustavsson, E. Mishin, E. Kendall, T. Mills, H. C. Carlson, and A. L. Snyder (2010), Creation of artificial ionospheric layers using high-power HF waves, *Geophys. Res. Lett.*, *37*, L02106, doi:10.1029/2009GL041895.

Shukla, P. K., L. Stenflo, and N. D. Borisov (1992), Nonlinear interaction of powerful radio waves with the plasma in the Earth's lower ionosphere, *J. Geophys. Res.*, *97*, 12,279, doi:10.1029/92JA00728.

Stenflo, L. (1985), Parametric excitation of collisional modes in the high-latitude ionosphere, *J. Geophys. Res.*, *90*, 5355, doi:10.1029/JA090iA06p05355.

Stubbe, P., H. Kopka, B. Thide, and H. Derblom (1984), Stimulated electromagnetic emission: A new technique to study the parametric decay instability in the ionosphere, *J. Geophys. Res.*, *89*, 7523, doi:10.1029/JA089iA09p07523.

Stubbe, P., H. Kohl, and M. T. Rietveld (1992), Langmuir turbulence and ionospheric modification, *J. Geophys. Res.*, *97*, 6285, doi:10.1029/91JA03047.

J. Battis, P. Kossey, and E. Mishin, Space Vehicles Directorate, Air Force Research Laboratory, AFRL/RVBXI, 29 Randolph Rd., Hanscom Air Force Base, MA 01731, USA.

S. Kuo, Department of Electrical and Computer Engineering, Polytechnic Institute of New York University, 6 MetroTech Center, Brooklyn, NY 11201, USA. (skuo@duke.poly.edu)

A. Snyder, NorthWest Research Associates, PO Box 530, Stockton Springs, ME 04981, USA.

REPORT DOCUMENTATION PAGE

1. REPORT DATE (DD-MM-YYYY)	2. REPORT TYPE	3. DATES COVERED (From - To)
03-03-2011	Reprint	

4. TITLE AND SUBTITLE

Ionospheric modification from under-dense heating by high-power HF transmitter

5a. CONTRACT NUMBER

5b. GRANT NUMBER

5c. PROGRAM ELEMENT NUMBER
62601F

6. AUTHORS

Spencer Kuo[*]
Arnold Snyder[**]
Evgeny Mishin
Paul Kossey
James Battis

5d. PROJECT NUMBER
1010   2301

5e. TASK NUMBER
HR   SD

5f. WORK UNIT NUMBER
ZZ   Z6

7. PERFORMING ORGANIZATION NAME(S) AND ADDRESS(ES)

Air Force Research Laboratory /RVBXI
29 Randolph Road
Hanscom AFB, MA 01731-3010

8. PERFORMING ORGANIZATION REPORT NUMBER

AFRL-RV-HA-TR-2011-1012

9. SPONSORING/MONITORING AGENCY NAME(S) AND ADDRESS(ES)

10. SPONSOR/MONITOR'S ACRONYM(S)
AFRL/RVBYB

11. SPONSOR/MONITOR'S REPORT NUMBER(S)

12. DISTRIBUTION/AVAILABILITY STATEMENT

Approved for Public Release; distribution unlimited.

13. SUPPLEMENTARY NOTES

14. ABSTRACT

Under-dense HF heating experiments were conducted near local solar noon as well as in the nighttime with the HF heater transmitting at 9.1 MHz directed along the geomagnetic zenith and run at 2 min on and 2 min. off. The effective isotropic radiated power of the HF transmitter exceeded 3 GW. The Digisonde operated in a fast mode that was used to monitor the temporal evolution of the ionospheric electron density distributions in the bottomside of the ionosphere (in the ranges from 90 to 190 km in the noontime and from 230 to 350 km in the nighttime. The electron temperature distributions were then evaluated. The results show that the electron density distributions are modified continuously over the experimental periods. In the noontime, the electron density decreases/increases in time in the region below/above a height at about 140 km, manifesting the change of the balance between the photoionization and the electron-ion recombination and the electron-oxygen dissociative attachment losses by the heating. In the nighttime, the ionosphere was lifted by 30 to 50 km through continuously upward expansion, resulting in the drop of the electron density in the bottomside of the ionosphere in time. A comparison with the ionogram, height, and electron density distribution of unheated ionosphere with similar background conditions further elaborates the observation of thermal expansion.

15. SUBJECT TERMS

Ionospheric modification   Inelastic collision   Electron dissociative attachment
Vibrational excitation   Ionosonde

16. SECURITY CLASSIFICATION OF:			17. LIMITATION OF ABSTRACT	18. NUMBER OF PAGES	19a. NAME OF RESPONSIBLE PERSON
a. REPORT	b. ABSTRACT	c. THIS PAGE			James Battis
UNCL	UNCL	UNCL	UNL	8	19B. TELEPHONE NUMBER (Include area code)